Journal of Engineering and Applied Sciences 12 (16): 4251-4258, 2017
ISSN: 1816-949X

Research of the Multi-Frequency Electrical Impedance Tomography using Possibility for Specific Physiological Processes Monitoring Tasks

G.K. Aleksanyan, A.I. Kucher and I.D. Shcherbakov
Department of Information and Measurement Systems and Technologies,
Platov South Russia State Polytechnic University (NPI), Novocherkassk, Russia

Abstract: The study is focused on development of computer finite element model of human chest using Femm and Octave S. The model has the geometry of an average person and takes into account the change in the conductivity and permittivity of biological tissues with increasing frequency of the injection current. The model allows the calculation of the value of the complex amplitude of the potential at any point of the object. A computational experiment, simulating the process of obtaining measurement data for electrical impedance tomography is described. An example of the simulation results and graphs of the complex amplitude of potentials on the surface of the object is considered. Using the method of multi-frequency electrical impedance tomography, BO structure with breathing and heart rate at different frequencies of the injected current was reconstructed. It was found that in the study of the internal structure of BO by EIT complex amplitude of the potential must be measured that allows to reconstruct the changes in both the real and imaginary parts of the complex conductivity BO carrying useful information. The results of these studies have shown that the method of multi-frequency EIT is an effective tool for visualization of the internal structures of BO and for monitoring and evaluation of dynamic (physiological) processes occurring in the BO. It is shown that it is possible to visualize the processes of respiration and heart rate using a different injected current frequency.

Key words: Multi-frequency electrical impedance tomography, the model, the direct problem, inverse problem, conductivity, dielectric constant and the heartbeat process, the process of breathing

INTRODUCTION

One of the promising areas of medical imaging is the Electrical Impedance Tomography (EIT) a method of imaging the internal structure of a Bbiological Object (BO) on the basis of non-invasive electrical measurements on its surface (Aleksanyan *et al*., 2014, 2016, 2015a-c). The method is as follows. Electrodes are applied on BO surface and are connected by a predetermined algorithm to injection current source. At the same time potential difference between the other electrodes are recorded. On the basis of the measurement information, the measurement algorithm and priori information about BO reconstruct the distribution of electrical conductivity in the BO with the application of mathematical methods for solving inverse problems. Thus, it is possible to visualize the internal structure of BO in the plane of the tomographic slice as well as obtain information about the dynamics of physiological processes occurring in the body. In carrying out an important role EIT frequency and current applied to the biological object. In this regard, research is needed to assess the effect of the injected current frequency as a result of the measurement and the result of the reconstruction (including the dynamic processes of monitoring tasks). Due to the fact that electrical properties depend on the frequency BO of the applied current, the use of multi-frequency EIT in clinical practice is an important tool for diagnostic information. For the development and research of the method of multifrequency EIT and its capabilities developed a two-dimensional finite-element computer model of the human chest. The research proposed model at different frequencies for the tasks of reconstruction and visualization of the area of man the lungs and the heart of man.

MATERIALS AND METHODS

For research of opportunities multifrequency EIT will be considered case of a two-dimensional finite element computer model of the human thoracic cage. As a tool for the development of the model selected Femm and mathematical computations environment Octave Software. Direct solution made in Femm (Meeker, 2015) which

Corresponding Author: G.K. Aleksanyan, Department of Information and Measurement Systems and Technologies, Platov South Russia State Polytechnic University (NPI), Novocherkassk, Russia

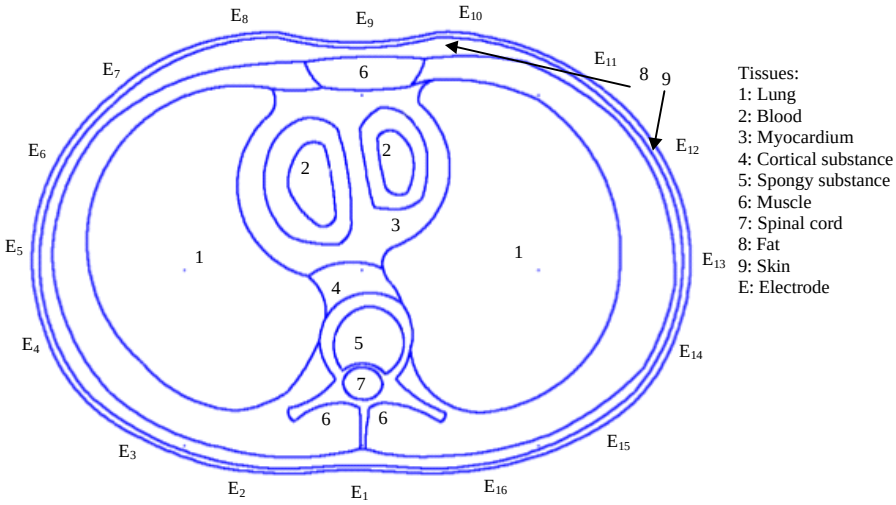

Fig. 1: Model tomographic section chest

Table 1: Relative permittivity ε biological tissues depending on f_i

	f_i (Hz)					
Tissue ε	10	100	1000	10^4	10^5	10^6
Lung	32×10^6	5.43×10^6	0.11×10^6	31×10^3	11513	1567
Muscle	3.03×10^7	9.11×10^6	5.99×10^5	2.63×10^4	8.37×10^3	1.68×10^3
Cortical substance	4.01×10^4	3.82×10^3	8.92×10^2	3.03×10^2	1.03×10^2	30.40
Spongy substance	ND	1.07×10^6	1.46×10^4	7.93×10^2	1.35×10^2	65.76
Spinal cord	3.56×10^7	3.20×10^6	1.54×10^5	1.60×10^4	3.03×10^3	7.24×10^2
Myocardium	7.1×10^6	0.85×10^6	0.31×10^6	0.10×10^6	14597	1584
Blood	3300	3200	3129	2700	2816	2010
Fat	1.02×10^7	3.51×10^5	7.88×10^3	2.70×10^2	32.23	14.03
Skin	0.77×10^6	0.41×10^6	0.19×10^6	0.11×10^6	27071	2925

consists of a set of programs for solving two-dimensional planar and axisymmetric problems. In solving the problem of currents spreading Femm solves the following equation (Meeker, 2015):

$$-(\sigma+j\omega\varepsilon)\nabla^2 V = 0$$

Where:

σ = Conductivity of the medium
ω = Angular frequency ($\omega = 2\pi f_i$)
ε = Dielectric constant of the medium
V = The scalar potential of the electric field

The geometry of the cross section of human chest is designed in an interactive shell Femm based tomographic image obtained by magnetic resonance imaging (Crabb *et al*., 2014; Happel *et al*., 2010) and is presented in Fig. 1. The outer dimensions of the model correspond to the size of an average adult. The model takes into account the presence of such human organs and tissues as the lungs, heart, muscle, spinal column, spinal cord, skin, fat and muscle tissue. At the same time, a number of assumptions and simplifications have been made in creating the model. For example, the parameters of the tissue at the borders do not change and are isotropic, absent pulmonary artery, trachea and esophagus are designated as areas filled with air, not marked ribs. However, we have developed detailed models is much higher than in the EIDORS models and in GREIT. The proposed model consists of heart infarction and two ventricles filled with blood.

To account for the heartbeat ventricular region is divided into two subregions. The outer subregion parameters vary from of the blood parameters to cardiac parameters. The outer boundary of the model at an equal distance from each other are 16 electrodes (the electrode radius -10 mm). The first electrode is located on the spine. Numbering of electrodes in a clockwise direction. For each material specified in the model conductivity σ and ε the permittivity of the material. The sources used. The frequency range for the parameters selected in the range of 10-1 MHz. For the material "skin" options damp skin were selected in which the voltage across the electrodes injecting no >9 which corresponds to the results of field experiments. The permittivity ε used for different frequency models of biological tissues is shown in Table 1. The electric conductivity σ of biological tissues used in the model for different frequencies shown in Table 2.

Table 2: The electrical conductivity σ of biological tissues depending on f_i

	f_i (Hz)					
Tissue (Sm/m)	10	100	1000	10^4	10^5	10^6
Lung on exhale	ND	1.39×10^{-1}	1.23×10^{-1}	1.42×10^{-1}	1.82×10^{-1}	2.02×10^{-1}
Lung on inhale	ND	4.16×10^{-2}	4.34×10^{-2}	4.97×10^{-2}	6.42×10^{-2}	6.47×10^{-2}
Muscle	1.96×10^{-1}	2.47×10^{-1}	2.97×10^{-1}	3.28×10^{-1}	3.63×10^{-1}	4.65×10^{-1}
Cortical substance	5.85×10^{-3}	5.86×10^{-1}	5.87×10^{-1}	5.89×10^{-1}	6.00×10^{-1}	7.00×10^{-1}
Spongy substance	ND	1.67×10^{-1}	1.72×10^{-1}	2.45×10^{-1}	2.44×10^{-1}	2.50×10^{-1}
Spinal cord	2.61×10^{-2}	7.07×10^{-2}	9.83×10^{-2}	1.11×10^{-1}	1.25×10^{-1}	1.52×10^{-1}
Myocardium	1.07×10^{-1}	1.12×10^{-1}	1.29×10^{-1}	1.81×10^{-1}	3.06×10^{-1}	5.06×10^{-1}
Blood	0.68	0.68	0.68	0.68	0.70	0.74
Fat	1.02×10^{-2}	1.62×10^{-2}	1.67×10^{-2}	1.72×10^{-2}	1.77×10^{-2}	1.83×10^{-2}
Skin	0.33	0.37	0.38	0.44	0.57	0.84

Mathematical computations environment Octave was chosen for the automatic modification of the model parameters problem. For each frequency f_I of $\sigma(f_I)$ and $\varepsilon(f_I)$ required values σ and e were selected which are accepted as the material parameters describing a particular biological tissue. In its absence, it is calculated by linear interpolation between the two closest points of the equation:

$$y = \frac{(y_{i+1}-y_i)f}{f_{i+1}-f_i} - \frac{(y_{i+1}-y_i)f_i}{f_{i+1}-f_i} + y_i$$

Where:

y = The desired value (σ or ε) for the frequency f

I = Array element number satisfying requirement $f_I \le f \le f_{i+1}$

f_i = Value of frequency f for which the specified value of the parameter y

Next drains and sources of the field are determined and the state of the electrodes is indicated. At the same time there are three state of the electrode-injecting (fixed current density $j \neq 0$), the electrode with zero potential (fixed potential U = 0) and the measuring electrode.

For the realization of computing experiment used the following sequence of actions (Fig. 2 is a schematic view of the first two dimensions). A1 electrode is electrode with zero potential, the electrode E2-injecting. The value of the potential on the electrodes E1..E16 φ_i is calculated. Further, the electrode E2 is connected as an electrode with zero potential, the electrode E3 and injecting a calculated value of the potential on the electrodes φ_i E1..E16 and so on until the electrode E16 is not designated as an electrode with zero potential and electrode E1 like injecting. For the data value computed potential difference $\Delta\varphi_i = \varphi_{i+1}-\varphi_i$ between the adjacent electrodes for each configuration injecting electrodes (Aleksanyan *et al*., 2015a-c).

Based on simulation results, the internal structure of the object of study was reconstructed and visualized using GREIT (Adler *et al*., 2009) (the differential reconstruction). For the first set of data taken into account the value and σ e lung exhalation, the outer contour of the heart ventricles assigned parameters

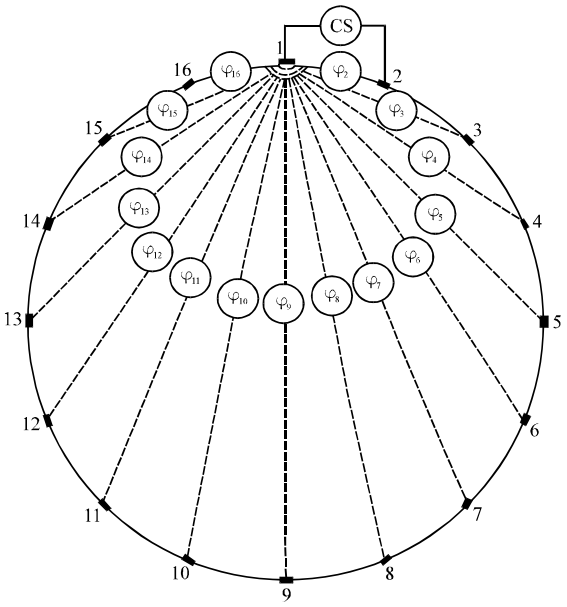

Fig. 2: Schematic representation of a method for producing measurement information

(σ and ε) infarction. For the sec set of data the parameters σand ε lung on inhalation, the outer contour of the heart ventricles are assigned to the parameters σ and ε blood. Thus, the processes of respiration and heart rate were taken into account in the study.

For the purposes of multi-frequency EIT sec data set is determined for f_I frequency different from the frequency of calculation of the first data set. This was reconstructed as the data obtained by simulating respiration and heartbeat as well as for data obtained at different frequencies at constant parameters σ and ε models (breath, heart in a relaxed state).

RESULTS AND DISCUSSION

Figure 3 and 4 shows a simulation result of measurement potentials φ_i by the above algorithm frequencies fI the injection current of 100 Hz; 1 kHz; 10 and 100 kHz and the amplitude/$_M$ = 5 mA for the real and

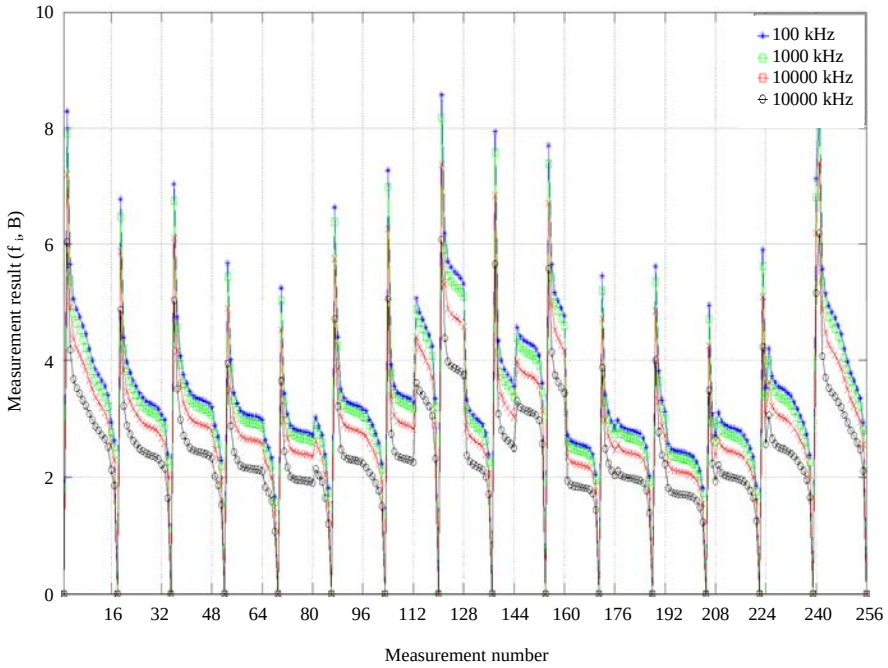

Fig. 3: The result of the simulation measurements f_i potentials (the real part of the complex amplitude of the signal)

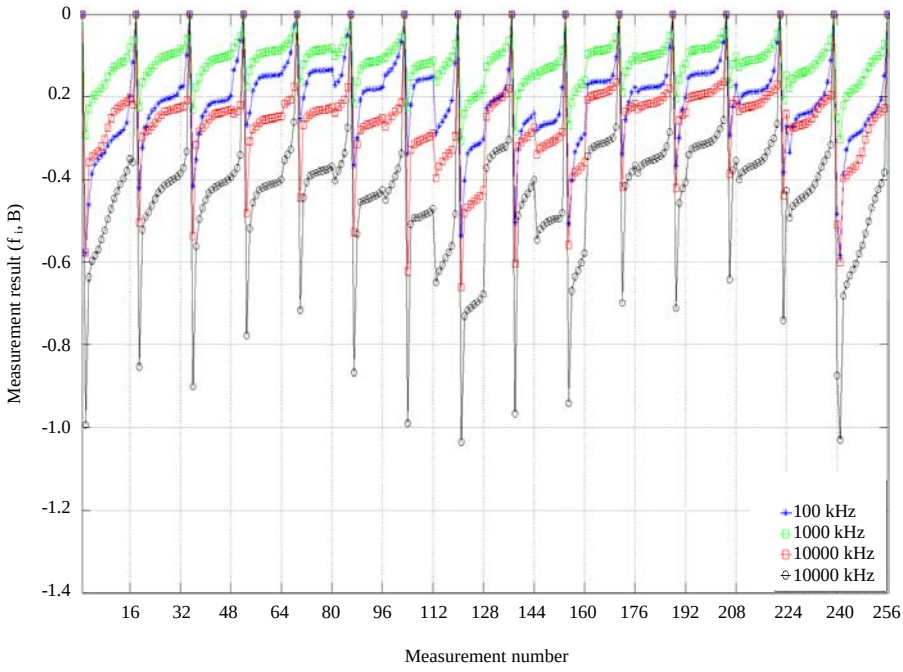

Fig. 4: The result of the simulation modeling measurement f_i potentials (the imaginary part of the complex amplitude of the signal)

imaginary parts of the signal. Figure 5 shows the result of calculation of the field distribution and potential directions of the currents in the model (the result of the direct problem solution) for 16 min while the configuration of the measuring electrodes f_I = 10 kHz and I_M = 5 mA. Figure 6 shows the result of reconstruction the BO internal structure in GREIT on a frequency of the injection current f_I equal to of 100 Hz; 1, 10, 100 and 500 kHz. For

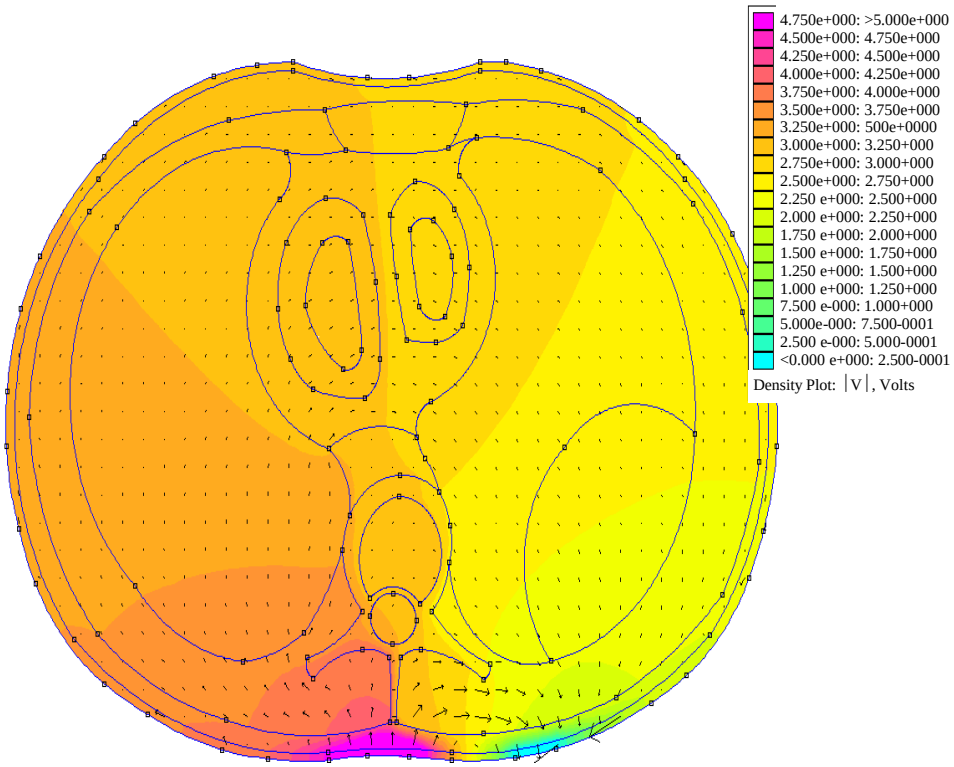

Fig. 5: The result of the direct problem in EIT Femm environment

the reconstruction adult_male_16el_lungs model of the libraries GREIT Models was used. The number of grid elements to solve the inverse problem N_{elem} = 587. Reconstruction settings is standard in accordance with the Adler *et al.* (2009). As in Fig. 6, at low f_I real component of conductivity is more contrasting picture and on higher frequencies-reactive (imaginary). Thus, from the results it can be concluded that the construction of a multi-frequency EIT system is necessary to measure the complex amplitude φ_i and reconstruct changes in both the real and the imaginary component of the complex conductivity.

Figure 7 shows the result of the reconstruction of real component of complex conductivity when simulating the processes of respiration and heartbeat. For the first data set f_I = 10 kHz, the data for the sec set value f_I varied from 20-100 kHz with steps of 10 kHz. As seen in Fig. 7 with the change f_I is possible to visualize a variety of physiological processes. So, when f_I = 20 kHz more contrast is the breathing process and at a frequency f_I = 70 kHz the heartbeat process. Figure 8 shows the result of the reconstruction of the imaginary component of the complex conductivity in GREIT when simulating respiration and heartbeat. For the first data set f_I = 10 kHz, the data for the sec set value f_I varied from 20-100 kHz with steps of 10 kHz. As in Fig. 8, in the reconstruction method of multi-frequency EIT imaginary component of the complex conductivity change f_I virtually no effect on the result of the reconstruction. Further research is necessary to extend the frequency range (Shaykhutdinov *et al.*, 2016).

Figure 9 shows the result of the reconstruction of the real component of the complex conductivity GREIT. The data were obtained at constant parameters of the model at different f_I. For the first data set f_I = 10 kHz, the data for the sec set value f_I varied from 20-100 kHz with steps of 10 kHz. As in Fig. 9, the reconstruction of the real component of the complex conductivity for a multi-frequency EIT assumes no useful information. Further research is needed in this area for the formation of a final decision.

Figure 10 shows the result of the reconstruction of the imaginary component of the complex conductivity in GREIT. The data were obtained at constant parameters of the model at different f_I. For the first data set f_I = 10 kHz, for a sec set of data f_I varied from 20-100 kHz with steps of 10 kHz. As in Fig. 10, the reconstruction of the imaginary component of the complex conductivity at high multifrequency EIT fI allows to distinguish between the internal organs. The chosen frequency range to the reconstruction clearly visible heart.

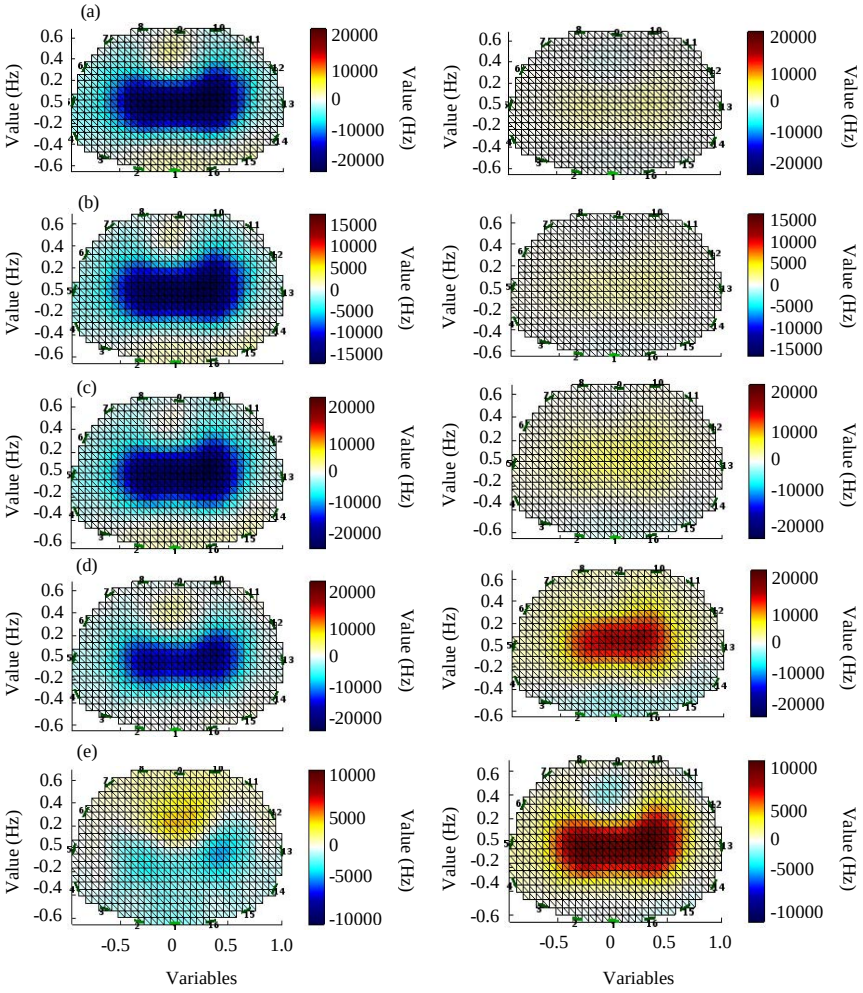

Fig. 6: The result of the reconstruction and visualization of the real (the real) and imaginary (Imag) part of the complex conductivity for frequency f_i equal to 100 Hz: a) 1 kHz; b) 10 kHz; c) 100 kHz; d) and 500 kHz and e) a tomographic slice chest

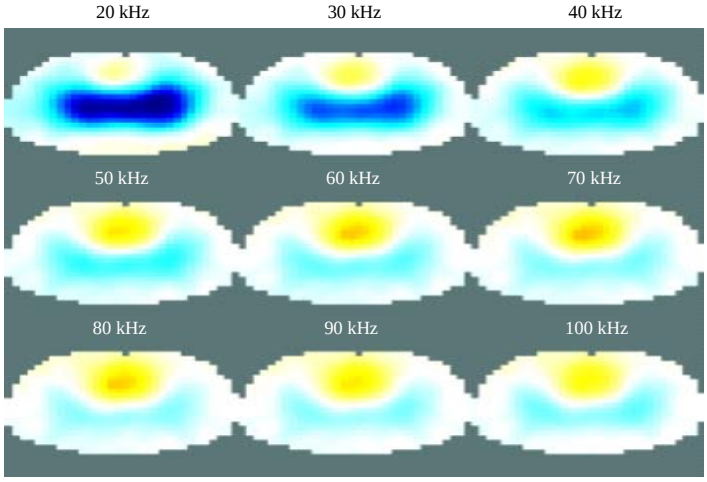

Fig. 7: Reconstruction and visualization of the real component of the complex conductivity when simulating the processes of respiration and heartbeat

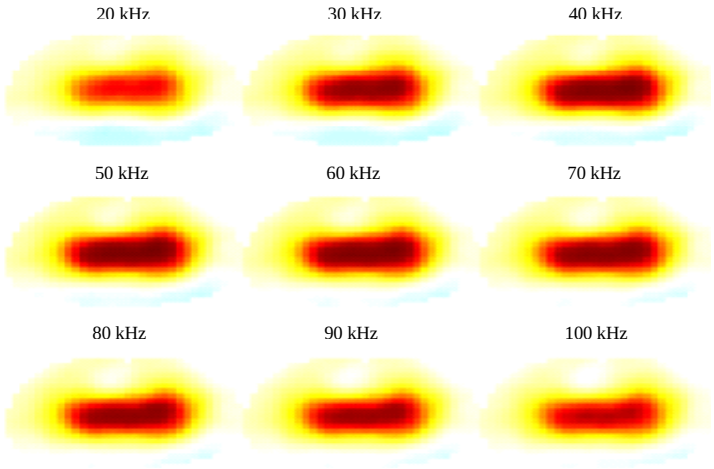

Fig. 8: Reconstruction and visualization of the imaginary component of the complex conductivity for simulating the processes of respiration and heartbeat

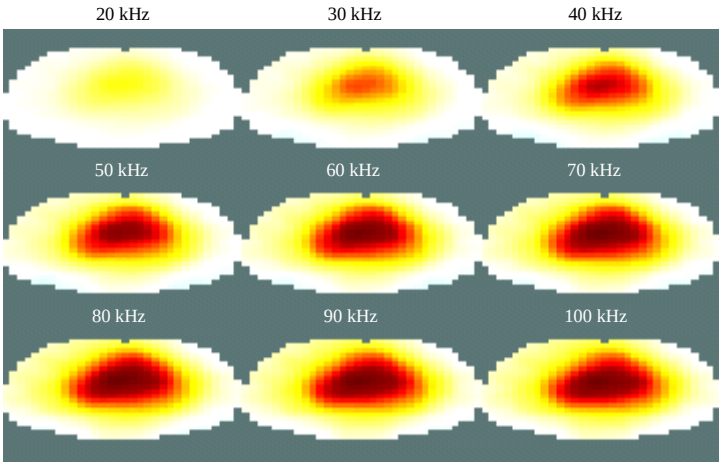

Fig. 9: Reconstruction and visualization of the real component of the complex conductivity in the area of the chest tomographic

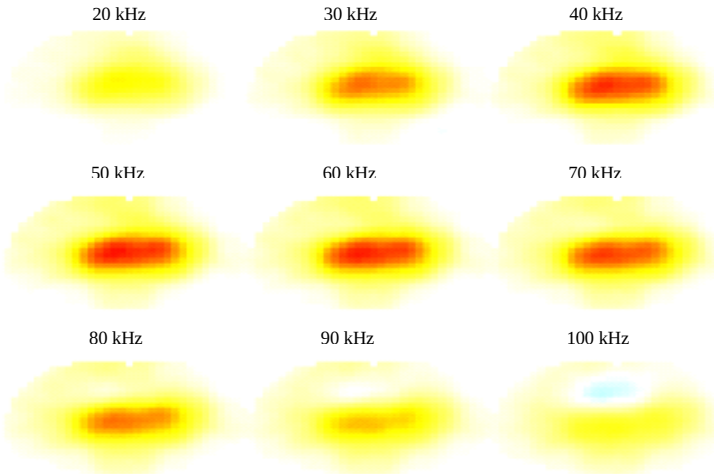

Fig. 10: Reconstruction and visualization of the imaginary component of the complex conductivity in tomographic chest

CONCLUSION

Computer finite element model of human was developed with Femm and Octave during this research. The model has the geometry of an average person and takes into account the change in the conductivity and permittivity of biological tissues with increasing frequency of the injection current. The model allows the calculation of the value of the complex amplitude of the potential at any point of the object.

Using the method of multi-frequency electrical impedance tomography structure inside the BO with breathing and heart rate at different frequencies was reconstructed. In the study of the internal structure of BO by EIT it was found that complex amplitude of the potential should be measured that allows to reconstruct the changes in both the real and imaginary parts of BO complex conductivity carrying useful information.

In addition, the research results showed that the method of multi-frequency EIT is an effective tool for visualization of the internal structures of BO and for monitoring and evaluation of dynamic (physiological) processes occurring in the BO. It is shown that it is possible to visualize the processes of respiration and heart rate using a different injected current frequency.

ACKNOWLEDGEMENTS

This research was supported by the Russian Foundation for Basic Research, Grant No. 16-38-60173 "Technology mining electrical impedance tomography for three-dimensional reconstruction and visualization of the conductivities of the internal structures of biological objects".

REFERENCES

Adler, A., J.H. Arnold, R. Bayford, A. Borsic and B. Brown *et al*., 2009. GREIT: A unified approach to 2D linear EIT reconstruction of lung images. Physio. Meas., 30: S35-S55.

Aleksanyan, G.K., A.I. Kucher, A.D. Tarasov, N.M. Chuong and C.N. Phong, 2015a. Design of software and experimental setup for reconstruction and visualization of internal structures of conductive bodies. Intl. J. Soft Comput., 10: 462-467.

Aleksanyan, G.K., N.I. Gorbatenko, A.I. Kucher, K.M. Shirokov and C.N. Phong, 2015b. Developing principles and functioning algorithms of the hardware-software complex for electrical impedance tomography of biological objects. Biosci. Biotechnol. Res. Asia, 12: 709-718.

Aleksanyan, G.K., N.I. Gorbatenko and A.I. Kucher, 2015c. Development and production of multi-layered electrode system for electrical impedance tomography devices. Int. J. Appl. Eng. Res., 19: 40580-40584.

Aleksanyan, G.K., N.I. Gorbatenko, D.A. Tarasov, 2014. Modern trends in development of electrical impedance tomography in medicine. Biosci. Biotechnol. Rese., 11: 85-91.

Aleksanyan, G.K., N.I. Gorbatenko, V.V. Grechikhin, T.N. Phong and T.D. Lam, 2016. Application of natural and model experiment methodology in two-dimensional electrical impedance tomography. ARPN. J. Eng. Appl. Sci., 11: 5871-5875.

Crabb, M.G., J.L. Davidson, R. Little, P. Wright and A.R. Morgan *et al*., 2014. Mutual information as a measure of image quality for 3D dynamic lung imaging with EIT. Physiol. Meas., 35: 863-879.

Happel, C.M., C. Klose, G. Witton, G.L. Angrisani and S. Wienecke *et al*., 2010. Non-destructive, high-resolution 3-dimensional visualization of a cardiac defect in the chick embryo resembling complex heart defect in humans using micro-computed tomography. Circulation, 122: e561-e564.

Meeker, D., 2015. Fenite Element Method Magnetics. Users's Manual Publisher, Singapore, Asia, Pages: 161.

Shaykhutdinov, D., D. Shurygin, G. Aleksanyan, I. Grushko and R. Leukhin *et al*., 2016. Analysis and synthesis of algorithms of solving inverse problems by methods of classical and modern automatic control theory. Asian J. Inf. Technol., 15: 1443-1446.